Microcalorimetric studies of interactions of ethene, isobutene, and isobutane with silica-supported Pd, Pt, and PtSn

M.A. Natal-Santiago, S.G. Podkolzin, R.D. Cortright and J.A. Dumesic *

Department of Chemical Engineering, University of Wisconsin, Madison, WI 53706, USA

Received 5 February 1997; accepted 25 March 1997

Microcalorimetric measurements were made of the interaction of hydrogen, ethene, isobutene and isobutane at 300 K with silica-supported Pt, Pd, and PtSn catalysts. The initial heats of hydrogen adsorption on silica-supported Pd and Pt are 104 and 95 kJ/mol, respectively. The presence of Sn decreases the saturation uptake of hydrogen on the PtSn sample. The initial heats of ethene interaction with Pd/silica and Pt/silica are 170 and 145 kJ/mol, respectively. The presence of Sn decreases the initial heat to 115 kJ/mol on the PtSn sample. The initial heats of isobutene interaction with silica-supported Pd and Pt are 160 and 190 kJ/mol, respectively. The presence of Sn decreases the initial heat to 125 kJ/mol on the PtSn sample. It appears that ethene and isobutene adsorb dissociatively on silica-supported Pd and Pt to form alkylidyne species at 300 K, with an average strength of carbon–metal bonds for these species near 230 kJ/mol. Ethene and isobutene adsorb on silica-supported PtSn to form di-σ- and π-bonded alkene species at 300 K, with an average strength of carbon–metal bonds for these species near 190 and 130 kJ/mol, respectively. Isobutane appears to adsorb dissociatively on a small number of sites on silica-supported Pd and Pt, and this dissociation is also inhibited by Sn on PtSn samples.

Keywords: hydrogen, ethene, isobutene, isobutane, palladium, platinum, microcalorimetry, density-functional theory

1. Introduction

Metal catalysts, such as supported platinum and palladium, are used extensively in the petrochemical and chemical industries for reactions such as the hydrogenation and dehydrogenation of hydrocarbons [1]. These metals may be supported on acidic supports to form bifunctional hydrocarbon reforming catalysts or the metals may be modified through the addition of promoters to influence hydrocarbon reactivity. A better understanding of the factors that control the strengths of interaction of hydrocarbons with these metal catalysts would assist the development of newer generations of metal catalysts with higher selectivities needed for more environmentally benign processes.

The interactions of light alkenes with metal surfaces have been studied in numerous investigations (e.g, see refs. [2–5] and references therein). For example, the adsorption of ethene on platinum has been investigated extensively over various crystal faces at different temperatures. These investigations have shown several distinct surface species, depending on temperature [6]. On Pt(111) surfaces, it was found that ethene is π-bonded to platinum at temperatures below 52 K [7], it is di-σ-bonded between 52 and 240 K [6], and it undergoes dehydrogenation to ethylidyne above 240 K [8]. Studies at temperatures near 200 K also suggest that π-adsorption is more stable on Pd surfaces, whereas di-σ-adsorption is preferred on Pt surfaces [5]. Light alkanes generally adsorb reversibly and weakly on close-packed surfaces at low temperatures (e.g., 200 K). Dissociative adsorption of *n*-butane has also been observed on the reconstructed Pt(110)-(1 × 2) surface at 200 K with a saturation coverage of $\sim$ 6% [9]. The geometry of the surface appears to exert a strong influence on the activation of C–H bonds in alkanes. Finally, the strength of interaction of alkenes with single-crystal surfaces has been measured by various investigators using temperature-programmed desorption [10–14]. Recently, King and co-workers [15] have used a single-crystal calorimeter to measure the heats of interactions of ethene on platinum at room temperature.

In the present study, we have employed heat-flow microcalorimetry to determine the strengths of interaction of ethene, isobutene, and isobutane with silica-supported Pt, PtSn, and Pd catalysts. These catalysts were chosen because they have different selectivities for the conversion of isobutane at temperatures near 673 K. In particular, PtSn is selective for isobutane dehydrogenation; Pt catalyzes dehydrogenation, hydrogenolysis, and isomerization; and Pd catalyzes dehydrogenation and hydrogenolysis, but shows low activity for skeletal isomerization. While heat-flow microcalorimetry has been used widely in the literature to study the adsorption of hydrogen and carbon monoxide on various metal surfaces [16,17], relatively fewer studies have been conducted of the interactions of light hydrocarbons with metal catalysts [15,18]. Finally, theoretical calculations using density-functional theory (DFT) were performed to complement the microcalorimetric measurements by

* To whom correspondence should be addressed.

providing energetics for the formation of hydrocarbon fragments prior to their adsorption on the surfaces of Pd and Pt.

2. Methodology

2.1. Preparation of samples

Samples containing 1.08% Pd and 2.5% Pt (analyzed by Galbraith Laboratories, Inc.) supported on Cab-O-Sil were prepared by ion-exchange of $M(NH_3)_4^{2+}$ with protons on the surface of silica, where M symbolizes Pd or Pt [19]. The degree of exchange was controlled by maintaining the pH of the slurry at ~ 7.6 by periodic addition of a solution of $M(NH_3)_4(OH)_2$. The resulting material was filtered, washed with deionized water, and dried overnight in air at 393 K. Samples of PtSn/silica containing 2 : 1 and 2 : 3 Pt/Sn molar ratios (Galbraith Laboratories, Inc.) were prepared via the evaporative impregnation of a solution of tributyltinacetate in methanol onto the 2.5% Pt/silica sample. The resulting materials were dried overnight in air at 393 K.

Prior to microcalorimetric studies, the samples were calcined under a flow of $\sim 10\%$ O_2/He for 2 h at 573 K, heating at a rate of ~ 4 K/min. The samples were cooled to room temperature, treated further under a flow of $\sim 10\%$ H_2/He for 2 h at 673 K, heating at a rate of ~ 2 K/min, and then stored in vials for further use.

2.2. Microcalorimetric measurements

Microcalorimetric measurements were performed at 300 K by using a Tian-Calvet heat-flow microcalorimeter (Seteram C80) connected to a calibrated dosing system. A detailed description of the apparatus can be found elsewhere [20,21]. A base pressure of 10^{-5} Torr and leak rates of the order of 10^{-6} Torr/min were typically obtained. Ethene, isobutene, and isobutane were purchased from Matheson with purity levels of $\sim 99.5\%$. These gases were purified further by performing freeze–pump–thaw cycles prior to each experiment. A capacitance manometer (Baratron, MKS Instruments) was used to measure the pressure of the probe molecules over the samples.

The number of Pd and Pt surface atoms on each catalyst was determined by chemisorption of hydrogen at 403 K, assuming that one hydrogen atom is associated with each surface metal atom at saturation coverage. Hydrogen (Liquid Carbonic) was purified for these measurements by passage through a Deoxo unit (Engelhard), followed by molecular sieves (Davison) in a bath of liquid nitrogen.

In a typical experiment, 0.5–1 g of sample was first outgassed at 393 K until the base pressure reached 10^{-3} Torr, and then evacuated at 673 K for 1 h, heating to the desired temperatures over periods of 1 h each. After cooling to room temperature, the sample was reduced in 400 Torr of hydrogen at 723 K for 2 h, heating to the final temperature over a period of 2 h. The gas inside the cells was evacuated and replaced at least three times during these reductions. The sample was next outgassed at 673 K for 2 h and subsequently allowed to cool to room temperature. The number of surface metal atoms was then determined via hydrogen chemisorption at 403 K. Afterwards, the sample was outgassed for 2 h at 673 K and subsequently cooled to room temperature. The microcalorimetric cells were then placed in the thermal block, and microcalorimetric measurements were initiated after the cells had equilibrated with the calorimeter at 300 K (typically overnight).

2.3. DFT calculations

Theoretical calculations were performed on the basis of density-functional theory (DFT), using the three-parameter functional B3LYP [22] along with the basis set 6-31+G* [23]. Detailed information about the theory can be found elsewhere [24,25]. The DFT calculations were performed using the software package GAUSSIAN 94® [26] on IBM SP2 and RS/6000 computers. Structural parameters for ethene, isobutene, and hydrocarbon radicals of interest were determined by optimizing to stationary points on the corresponding potential-energy surface using the Berny algorithm and redundant internal coordinates [27]. Optimization criteria consisted of maximum forces and displacements of less than 2.2 kJ/(mol Å) and 0.0010 Å, respectively, in addition to root-mean-squared forces and displacements of less than 1.5 kJ/(mol Å) and 0.0006 Å. The resulting molecular structures were classified as local minima on the potential-energy surface by calculating the Hessian matrix analytically and ensuring that its eigenvalues were all positive [28]. The vibrational frequencies obtained from the analysis of force constants were used further without scaling to estimate thermochemical properties for the aforementioned hydrocarbons at 300 K.

2.4. Reaction kinetics studies

Reaction kinetics studies of isobutane conversion were conducted using a quartz, down-flow reactor. Helium (Liquid Carbonic) was employed as a carrier gas, purified by passage over reduced Oxytrap (Alltech) at 298 K, followed by activated molecular sieves (13X) at 77 K. Isobutane (Liquid Carbonic, 99.5%) was treated by passage over beds of reduced Oxytrap (Alltech) and reduced Ni on alumina at 373 K to remove oxygen and sulfur impurities, respectively. Hydrogen (Liquid Carbonic) was treated by passage through a Deoxo unit (Engelhard) and a bed of molecular sieves (13X) at 77 K. The reactor inlet and outlet gases were analyzed by a HP-5890 gas-chromatograph with FID detector and a

20 foot 15% Squalane Chromsorb PAW column held at 323 K. Turnover frequencies were calculated from the kinetic data by normalizing the rates to the number of surface metal atoms determined by the saturation uptakes of hydrogen at 403 K. These kinetics studies were conducted using sieved fractions (80–120 mesh) of the various silica-supported catalysts at reaction conditions of 673 K, 12.5 Torr of isobutane, 75 Torr of hydrogen and a total pressure of 760 Torr. All catalysts were first reduced with hydrogen at 773 K for 1 h and then cooled to 673 K before kinetic data were collected.

3. Results and discussion

3.1. Hydrogen adsorption

Microcalorimetric data for the dissociative chemisorption of hydrogen on silica-supported Pd and Pt are plotted in figure 1 as the differential heat of adsorption versus H-coverage. For convenience, the differential heat is defined as the negative of the differential change in enthalpy for the adsorption processes. The initial heats of hydrogen adsorption on silica-supported Pd and Pt are 104 and 95 kJ/mol, respectively, with an absolute error of 5 kJ/mol. These heats correspond to metal–hydrogen bond strengths of 266 and 270 kJ/mol on Pt and Pd, respectively. The saturation H-coverage for 1.08% Pd and 2.5% Pt supported on silica is $\sim$ 110 μmol/g in each case, which corresponds to metal dispersions of approximately 100 and 86%. The effect of Sn on the adsorption of hydrogen on Pt/silica is not included here, but the primary effect of Sn is to decrease the saturation uptake as reported elsewhere [29]. In particular, the saturation H-coverages were 52 and 33 μmol/g for the samples with 2 : 1 and 2 : 3 Pt/Sn molar ratios, respectively.

The results from this study of hydrogen chemisorption are in agreement with previous calorimetric investigations of Pt/silica [29] and Pd/silica [30], for which heats of H_2 adsorption of 93 and 100 kJ/mol have been reported, respectively, on samples with high metal dispersions. In addition, it can be seen that the differential heat of adsorption of hydrogen on palladium does not decrease to zero near the saturation coverage. We may attribute this phenomenon to the formation of a bulk hydride phase (PdH_x), whose absolute heat of formation has been reported to be less than 20 kJ/mol [31].

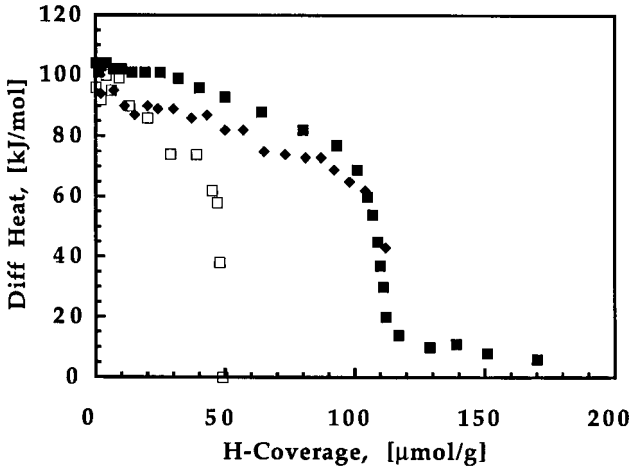

Figure 1. Differential heat versus H-coverage for the dissociative adsorption of hydrogen at 403 K on silica-supported, 1.08% Pd (■), 0.85% Pt (□), and 2.5% Pt (◆).

3.2. Ethene adsorption

Microcalorimetric data for the interaction of ethene with silica-supported Pd and Pt are shown in figure 2. Two independent experiments for Pd/silica are shown to demonstrate the reproducibility of the measurements, for which the absolute error is less than 10 kJ/mol. The heat of ethene adsorption on silica has been included to show when the metal surface is saturated. The absolute coverage of the hydrocarbon has been normalized by the saturation coverage of H-adatoms from figure 1 to allow for the comparison of results from different samples on the basis of the number of surface metal atoms.

The initial heat of ethene interaction with Pt/silica is 145 kJ/mol, remaining constant to a coverage of $\sim$ 10%, after which it decreases until saturation is reached at a coverage of $\sim$ 22%. These results are in agreement with previous studies in which an initial heat of 150 kJ/mol and a saturation coverage of $\sim$ 18% were reported [29]. The initial interaction of ethene with Pt/silica most likely leads to the formation of ethylidyne species ($M_3{\equiv}CCH_3$) [5]. However, one should be cautious when examining the trend of adsorption energies versus surface coverage given that the sticking coefficients for alkenes on metals are high and adsorption is

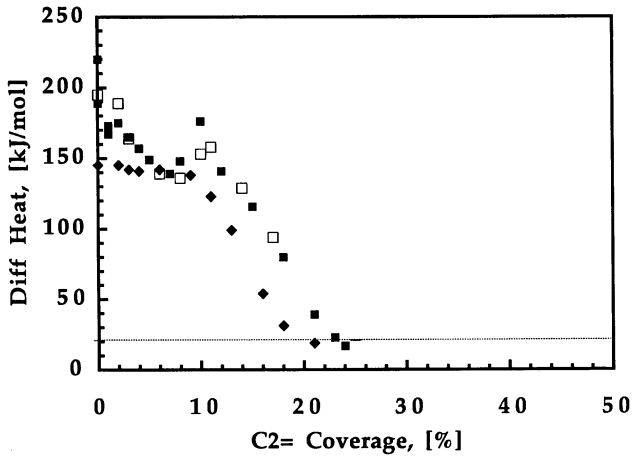

Figure 2. Differential heat versus relative coverage for the adsorption and reaction of ethene on silica-supported, 1.08% Pd (■ = #1; □ = #2) and 2.5% Pt (◆), in addition to silica (——), at 300 K. The absolute hydrocarbon coverages have been normalized by the saturation H-coverages from figure 1.

largely irreversible. It is possible that for our measurements each adsorption pulse saturates different parts of the sample. The saturation coverage determined by our studies is consistent with an ensemble size of 5 or 6 Pt-atoms for the decomposition of ethene, as suggested previously [32].

Single-crystal, microcalorimetric measurements of ethene interaction with Pt(110)-(1 × 2) at 300 K have been interpreted in terms of species with heats of reaction of 205, 170, 136, and 120 kJ/mol (with an absolute error of 8 kJ/mol), suggested by the investigators to be ethylylidyne ($M_3{\equiv}CCH_2$–M), ethylidyne, di-σ-, and π-adsorbed species, respectively [15]. The ethylylidyne species were present at very low coverages, and it is possible that these species were not detected in our measurements due to their low concentration. It appears that our initial heat of 145 kJ/mol may reflect an average of the values for ethylidyne and di-σ-adsorbed ethene species.

Results for the interaction of ethene with samples of PtSn/silica are shown in figure 3, with duplicate runs included for the 2 : 1 Pt/Sn sample to demonstrate the reproducibility of the measurements, for which the absolute error is less than 5 kJ/mol. The presence of Sn decreases the initial heat of ethene adsorption to 115 kJ/mol. The saturation coverage of ethene on the silica-supported PtSn increases from ~ 34 to ~ 42% as the content of Sn increases from 2 : 1 to 2 : 3 Pt/Sn molar ratio. Modification of the Pt surface with Sn results in the inhibition of the dissociative adsorption of ethene, caused by a decrease in the size of the surface ensembles [29]. A heat of adsorption equal to 115 kJ/mol is consistent with π- and/or di-σ-adsorbed ethene, as seen for ethene adsorption on Pt powder at 173 K [5,33]. Previous desorption and spectroscopic studies of ethene adsorption on ordered Sn/Pt(111) surface alloys also support the proposed formation of di-σ-bonded species on the PtSn/silica samples [34].

The initial heat of ethene interaction with Pd/silica may be as high as 220 kJ/mol; however, the heat of interaction decreases to ~ 170 kJ/mol as the low coverage of 1% is approached, and the heat of interaction decreases almost to 140 kJ/mol as the coverage reaches ~ 8%. This high initial heat may be caused by the formation of highly-dehydrogenated hydrocarbon fragments at very low coverages, most likely ethylylidyne species, as suggested [15] for ethene adsorption on Pt(110)-(1 × 2) at 300 K. Ethylidyne species are expected to form at the higher coverages ranging from 1 to 8%. In the 8–12% range of coverages, the heat of interaction is observed to increase and pass through a maximum of 160–180 kJ/mol. This behavior is probably caused by the hydrogenation of ethene by adsorbed hydrogen atoms, leading to the production of ethane, which has been detected in the gas phase in independent studies performed in our group [33]. At coverages higher than 12%, the heat of interaction decreases until a saturation coverage of ~ 22% is reached.

3.3. Isobutene adsorption

Microcalorimetric data for the interaction of isobutene with silica-supported Pd, Pt, and PtSn are shown in figure 4. To aid in the discussion of the results, schematic drawings of possible hydrocarbon products of the interaction of isobutene with metal surfaces are included in figure 5. The initial heats of isobutene interaction with silica-supported, 1.08% Pd and 2.5% Pt are 160 and 190 kJ/mol, with saturation coverages of ~ 8 and ~ 5%, respectively.

Various spectroscopic studies have been conducted

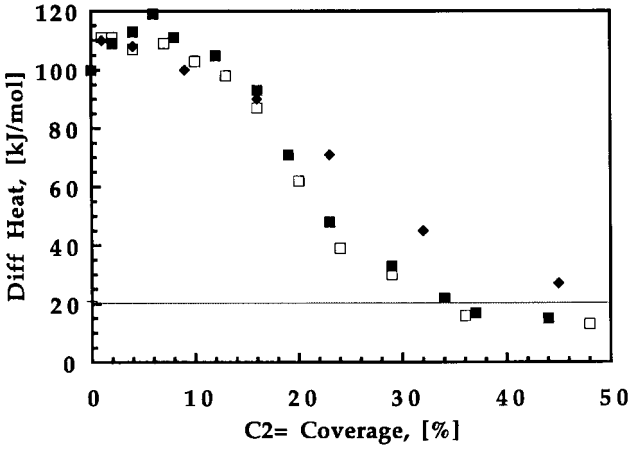

Figure 3. Differential heat versus relative coverage for the adsorption of ethene on silica-supported 2 : 1 Pt–Sn (■ = #1; □ = #2) and 2 : 3 Pt–Sn (◆), in addition to silica (——), at 300 K. The absolute hydrocarbon coverages have been normalized by the saturation H-coverages from figure 1.

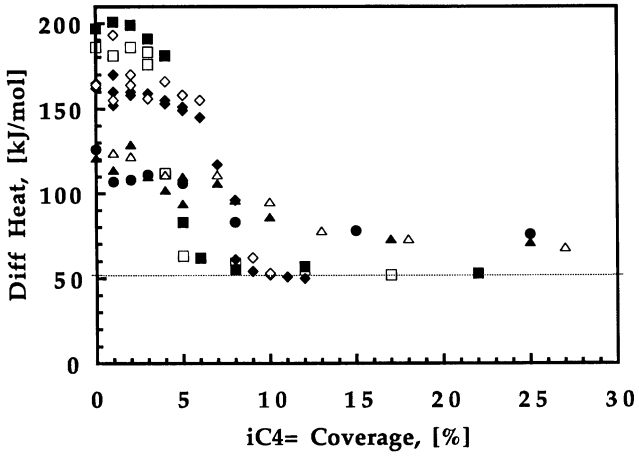

Figure 4. Differential heat versus relative coverage for the adsorption of isobutene on silica-supported 1.08% Pd (◆ = #1; ◇ = #2), 2.5% Pt (■ = #1; □ = #2), 2 : 1 Pt–Sn (▲ = #1; △ = #2), and 2 : 3 Pt–Sn (●), in addition to silica (——), at 300 K. The absolute hydrocarbon coverages have been normalized by the saturation H-coverages from figure 1.

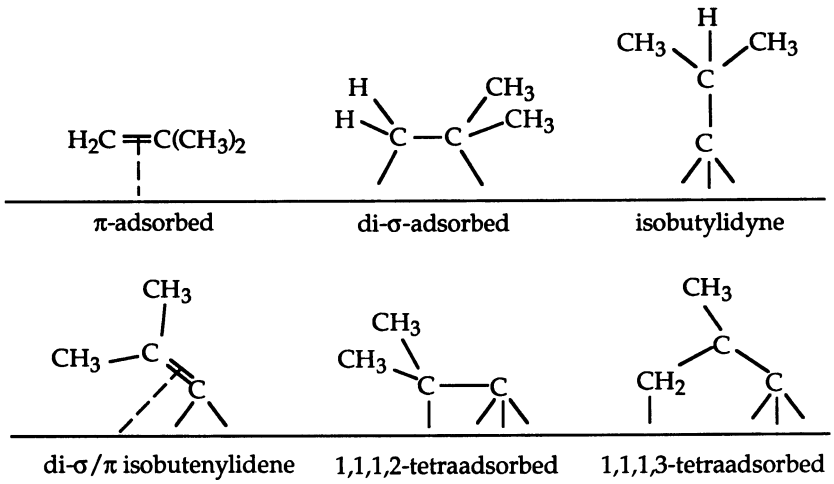

Figure 5. Schematic drawings of possible hydrocarbon products of the adsorption and reaction of isobutene on metal surfaces.

of the interaction of isobutene with Pt(111) [35,36] and on polycrystalline surfaces of silica-supported Pd [37] and Pt [38]. At temperatures lower than 200 K, isobutene is di-σ-bonded to metal surfaces, with π-character in some cases. Upon heating to room temperature, adsorbed isobutene decomposes to form adsorbed hydrogen atoms and isobutylidyne, mixed with π- and di-σ-bonded species. Above 300 K, substantial loss of hydrogen from the adspecies is observed, leading to the formation of more highly-dehydrogenated fragments.

By analogy with our results for the formation of ethylidyne species on silica-supported Pd and Pt (see figure 2), it appears that isobutylidyne species are formed from isobutene on Pd/silica at 300 K. In contrast, the high initial heat of interaction for isobutene with Pt/silica is evidence for the formation of adspecies with a lower H/C ratio than isobutylidyne. Previous HREELS measurements for the adsorption and reaction of isobutene on Ni(111) were interpreted in terms of di-σ-adsorbed species which decompose near room temperature to tilted, triply-coordinated di-σ-/π-adsorbed isobutenylidene species [39]. Alternatively, 1,1,1,2- or 1,1,1,3-tetraadsorbed species may be possible adsorbed species. In general, the adsorption of an extra hydrogen atom on Pt accompanied by the formation of another carbon–metal bond would account for a higher heat of formation of these species on Pt compared to formation of isobutylidyne species. The lower saturation coverage for isobutene on Pt/silica compared to Pd/silica may be caused by a requirement for specific adsorption sites, steric effects, and/or adsorption of the extra hydrogen atoms on Pt/silica. The formation of more highly dehydrogenated C_4-fragments on Pt than on Pd may be related to the greater radial expansion of the Pt d-orbitals compared to those of Pd. Accordingly, it may be easier for Pt surfaces to accommodate four carbon–metal bonds, as in the case of 1,1,1,2- or 1,1,1,3-tetraadsorbed species, than for Pd surfaces at room temperature.

Microcalorimetric data for the interaction of isobutene with PtSn/silica are presented in figure 4. The initial heat of isobutene interaction with the 2 : 1 and 2 : 3 Pt–Sn/silica samples is 125 kJ/mol. The primary effect of Sn on the interaction of isobutene with Pt/silica is, as in the case of ethene, to inhibit the formation of products of dissociative adsorption by decreasing the size of Pt surface ensembles. The heterogeneity of the differential heat curve suggests that π- and di-σ-adsorbed isobutene species are both present.

3.4. Isobutane adsorption

Previous studies of isobutane interaction with Pt(111) and Sn/Pt(111) have shown the adsorption to be weak and reversible at temperatures below 150 K [40]. On an open surface such as Pt(110)-(1 × 2), isobutane adsorbs dissociatively at 335–630 K [41]. Microcalorimetric results for the interaction of isobutane with silica-supported Pd, Pt, and PtSn are shown in figure 6. Unfortunately, it was not possible to obtain reproducible values of the initial heats for isobutane interaction with silica-supported Pd and Pt, as shown by the two trials included in figure 6 for Pt/silica. The initial heat of isobutane interaction appears to lie within the range of 160 to 225 kJ/mol, with saturation coverages of $\sim$ 4% for Pt/silica and $\sim$ 8% for Pd/silica. In both cases, the high initial heats are evidence for dissociative adsorption of isobutane, and the observed saturation coverages are probably related to the number of defect sites on the supported metal surfaces. The addition of Sn to Pt/silica, as in the previous cases of alkene adsorption, inhibits the dissociative adsorption of isobutane, reducing the saturation coverage to less than 2%.

3.5. DFT calculations

To estimate the strength of the carbon–metal bonds in the proposed surface species, DFT calculations were

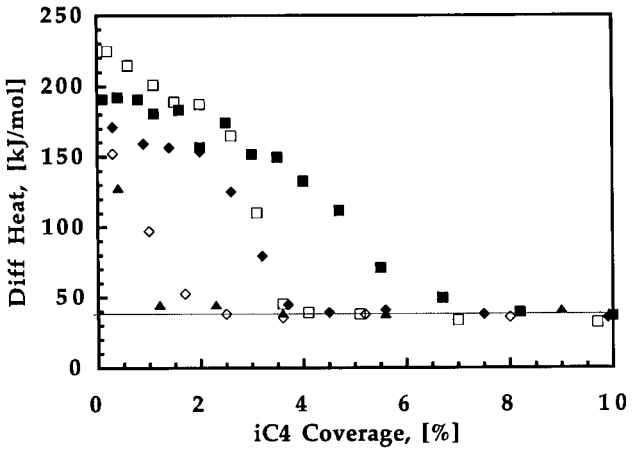

Figure 6. Differential heat versus relative coverage for the adsorption of isobutane on silica-supported, 1.08% Pd (■), 2.5% Pt (□ = #1; ◆ = #2), 2 : 1 Pt–Sn (◇), and 2 : 3 Pt–Sn (▲), in addition to silica (——), at 300 K. The absolute hydrocarbon coverages have been normalized by the saturation H-coverages from figure 1.

performed at the B3LYP/6-31+G* level for ethene, isobutene, isobutane, and the corresponding radicals of interest. The relevant energies of formation of several hydrocarbon radicals from the parent alkenes or alkane are included in table 1. In this table, the vibrational frequencies necessary for the estimation of the reported thermodynamic properties were estimated within the harmonic, quadratic approximation and used without further scaling. The gas-phase radicals presented in table 1 are those leading to adsorbed di-σ-bonded, ethylidyne, ethylylidyne, isobutylidyne, 1,1,1,2-tetraadsorbed-iso-C_4, and 1,1,1,3-tetraadsorbed-iso-C_4 species. Also, for "calibration" purposes, the predicted H–H bond strength, heat of ethene hydrogenation, and heat of isobutene hydrogenation have been included in table 1 and compared with accepted values.

It can be seen that the stability of the hydrocarbon radicals depends on the location of the unpaired electrons. For example, the ethylidyne radical CCH_3, which has three unpaired electrons in the same carbon atom, is less stable by ~ 40 kJ/mol than its isomer $CHCH_2$, which has the three unpaired electrons distributed between two carbon atoms. The predicted energies of formation of the radicals of interest can be combined with the measured heats of interaction to estimate the strengths of the bonds formed between carbon atoms in the hydrocarbon fragments and the metal surface. The experimental heats of reaction used for this purpose are included in table 2, along with the calculated, average carbon–metal bond strengths on silica-supported Pt and Pd corresponding to each assumed scenario in the table.

It follows from table 2 that the average strength of carbon–metal bonds must be less than 130 kJ/mol in π-bonded ethene, since this value is the highest heat measured for ethene adsorption on Pt and Pd at the low temperatures where only π-bonded and di-σ-bonded ethene are formed. Similarly, the average strength of carbon–metal bonds must be near 190 kJ/mol for di-σ-bonded ethene. From the initial heat of ethene adsorption at 300 K, where ethylidyne species are most likely formed, we can estimate the average strength of carbon–metal bonds to be near 230 kJ/mol for these ethylidyne species. Isobutene adsorption on Pd at 300 K also leads predominantly to isobutylidyne species, since the average carbon–metal bonds calculated from the initial heat correspond to values near 230 kJ/mol for this species (similar to the value for bonding of ethylidyne species). In the case of Pt, however, the higher initial heat of isobutene adsorption suggests that a more highly dehydrogenated species is formed, and the average carbon–metal bond strengths calculated from the initial heat correspond to values near 230 kJ/mol for these possible species.

Table 1
Estimation of changes in thermodynamic properties for the formation of various C_2 and C_4 radicals from ethene and isobutene on the basis of B3LYP/6-31+G*

Reaction at 298 K	ΔE (kJ/mol)	ΔH (kJ/mol)	ΔG (kJ/mol)	Accepted ΔH (kJ/mol)
$H_2 \rightarrow 2H$	434	436	407	436
$C_2H_4 + H_2 \rightarrow C_2H_6$ (staggered)	−139	−142	−106	−137
iso-$C_4H_8 + H_2 \rightarrow$ iso-C_4H_{10}	−113	−115	−78	−118
$C_2H_4 \rightarrow H_2\dot{C}\dot{C}H_2$	253	253	244	
$C_2H_4 \rightarrow \cdot\dot{C}HCH_3$	285	285	275	
$C_2H_4 \rightarrow H + \cdot\dot{C}H\dot{C}H_2$	754	756	715	
$C_2H_4 \rightarrow H + \cdot\dot{\dot{C}}CH_3$	794	797	756	
$C_2H_4 \rightarrow 2H + \cdot\dot{\dot{C}}\dot{C}H_2$	1 288	1 293	1 217	
iso-$C_4H_8 \rightarrow H_2\dot{C}\,\dot{C}(CH_3)_2$	255	255	247	
iso-$C_4H_8 \rightarrow H + \cdot\dot{\dot{C}}C(CH_3)_2H$	813	816	780	
iso-$C_4H_8 \rightarrow 2H + \cdot\dot{\dot{C}}\dot{C}(CH_3)_2$	1 255	1 260	1 187	
iso-$C_4H_8 \rightarrow 2H + \cdot\dot{\dot{C}}C(CH_3)(\dot{C}H_2)H$	1 232	1 237	1 165	

Table 2
Heats of reaction and corresponding metal–carbon bond strengths for the adsorption and reaction of ethene and isobutene on silica-supported Pd and Pt

	$-\Delta H$ (kJ/mol)	
	Pt	Pd
H_2	95	104
C_2H_4 (low temp.) [a]	120	130
C_2H_4	150	170
iso-C_4H_8	190	160
	M–C bond (kJ/mol)	
	Pt	Pd
M–H → M + H	266	270
Ethene		
M_2–C_2H_4 (di-σ) (low temp.)	**187** *	**192** *
M_2–C_2H_4 (di-σ)	202	212
M_3–CCH_3	**227** *	**232** *
Isobutene		
M_2–iso-C_4H_8 (di-σ)	223	208
M_3–$CC(CH_3)_2H$	247	**235** *
M_3–$CC(CH_3)_2$–M	**230** *	220
M_3–$CC(CH_3)H(CH_2)$–M	224	214

[a] Taken from ref. [33].
* Most probable scenario.

3.6. Kinetics of isobutane conversion

In agreement with results from previous studies [29], table 3 indicates that the addition of Sn to Pt/silica suppresses the production rates of methane, ethane, propane, and *n*-butane. The turnover frequencies for formation of hydrogenolysis and isomerizeration products are an order of magnitude lower over the PtSn/silica catalyst compared to the Pt/silica catalyst. The isobutane conversion over the highly selective PtSn/silica catalyst was limited by the equilibrium conversion of isobutane to isobutene which is 7% at the reaction condition.

Table 3 shows slightly higher production rates of methane, ethane, and propane (hydrogenolysis products) over Pd/silica compared to the Pt/silica catalyst. Importantly, the production rate of *n*-butane (isomerization product) is significantly lower over Pd/silica compared to Pt/silica. Anderson and Avery [42] reported a similar trend in the isomerization to hydrogenolysis ratio for platinum and palladium films.

It is generally accepted that hydrogenolysis reactions require the removal of at least several hydrogens from the alkane molecule, with the formation of a reactive surface intermediate which is bonded to the surface through multiple carbon–metal bonds [43–45]. In a similar fashion, the bond-shift mechanism suggested for the metal-catalyzed isomerization reaction of isobutane requires that the alkane molecule undergoes successive dehydrogenation steps before the rate-limiting bond-shift step. Anderson and Avery [42] suggested a bond-shift mechanism that proceeds through a 1,3 $\alpha\alpha\gamma$-triadsorbed intermediate bonded to two contiguous metal atoms. In this mechanism, a bond forms between the carbon atoms bonded to the surface, and one of the bonds in the resulting short-lived cyclopropane ring breaks to form an adsorbed straight-chain intermediate. This intermediate is then hydrogenated, followed by desorption from the surface as *n*-butane.

As discussed elsewhere, it has been suggested that Sn decreases the size of surface Pt ensembles, thereby inhibiting the formation on the surface of highly dehydrogenated hydrocarbon species required for hydrogenolysis, isomerization, and coking reactions [29,46]. This conclusion is supported by the microcalorimetric results in figures 2–4 which show that the addition of Sn to Pt/silica decreases the initial heat of ethene interaction from 145 to 115 kJ/mol, and it decreases the initial heat of isobutene interaction from 190 to 125 kJ/mol. As discussed above, it appears that ethene and isobutene interact with Pt/silica at 300 K to form ethylidyne and isobutylidyne species, whereas ethene and isobutene adsorb to form π- or di-σ-bonded species on PtSn/silica. Moreover, the microcalorimetric result that more highly dehydrogenated isobutene species form on Pt compared to Pd at 300 K is consistent with the higher rates of isobutane isomerization over Pt, since the reactive intermediates involved in isomerization are more highly dehydrogenated that those involved in hydrogenation–dehydrogenation reactions, and they may also be more highly dehydrogenated than those species involved in hydrogenolysis reactions.

4. Conclusions

(1) Ethene, isobutene, and isobutane adsorb dissociatively on silica-supported Pd and Pt at 300 K, whereas dissociation is negligible over PtSn/silica catalysts.

(2) Dissociative adsorption of ethene on Pt/silica and Pd/silica at 300 K leads predominantly to ethylidyne species (while a more highly-dehydrogenated fragment may also form at very low coverages on Pd/silica). The average strength of carbon–metal bonds for these ethylidyne species is near 230 kJ/mol.

(3) Dissociative adsorption of isobutene involves different surface species on silica-supported Pd and Pt. Isobutylidyne species appear to form on Pd/silica, whereas more highly-dehydrogenated species may also form on Pt/silica. The average strengths of carbon–metal bonds for isobutylidyne and these more highly dehydrogenated species are near 230 kJ/mol.

(4) Modification of Pt/silica with Sn results in the inhibition of the dissociative adsorption of ethene, isobutene, and isobutane. The average strength of carbon–

Table 3
Conversion of isobutane under reaction conditions of 673 K, 12.5 Torr isobutane, 75 Torr hydrogen

Catalyst	2 : 1 Pt–Sn/silica	2.5% Pt/silica	1.08% Pd/silica
WHSV [a]	7.4	9.7	7.7
isobutane conversion (%)	5.9	21.2	37.7
isobutane conversion TOF [b]	4.94×10^{-2}	9.87×10^{-2}	1.51×10^{-1}
CH_4 TOF [b]	2.03×10^{-3}	1.21×10^{-1}	3.52×10^{-1}
C_2H_6 TOF [b]	6.90×10^{-4}	1.77×10^{-2}	1.99×10^{-2}
C_3H_8 TOF [b]	3.49×10^{-4}	2.86×10^{-2}	4.21×10^{-2}
n-C_4H_{10} TOF [b]	1.76×10^{-3}	1.54×10^{-2}	2.38×10^{-3}
i-C_4H_8 selectivity [c]	94.2	23.0	12.9
ethane/methane	0.32	0.14	0.06
propane/methane	0.17	0.23	0.12
n-butane/methane	0.86	0.12	0.007

[a] WHSV = (g isobutane/h)/(g catalyst).
[b] TOF = (molecules of product)/(number of surface Pt × s).
[c] Selectivity = (100 × moles of product)/(moles of isobutane reacted).

metal bonds is near 190 kJ/mol for di-σ-adsorbed complexes, and lower than 130 kJ/mol for π-adsorbed species.

(5) The strengths of interaction of ethene, isobutene, and isobutane with the samples appears to correlate with catalytic activity. The addition of Sn to Pt weakens the interaction with these hydrocarbons by suppressing the extent of dehydrogenation and lowers the catalytic activity for hydrogenolysis and skeletal isomerization reactions. Palladium shows a weaker interaction with isobutene and isobutane compared to platinum, probably related to less extensive dehydrogenation, and exhibits lower catalytic activity for skeletal isomerization reactions.

Acknowledgement

The authors wish to acknowledge the financial support of the National Science Foundation, as well as the GEM fellowship awarded to MANS. The authors also would like to thank Professor J.J. de Pablo at University of Wisconsin-Madison for making available the computers and the software package used for the DFT calculations.

References

[1] B.C. Gates, J.R. Katzer and G.C.A. Schuit, *Chemistry of Catalytic Processes* (McGraw-Hill, New York, 1979) ch. 3.
[2] G.A. Somorjai, *Introduction to Surface Chemistry and Catalysis* (Wiley, New York, 1994).
[3] B.E. Bent and G.A. Somorjai, Adv. Coll. Inter. Sci. 29 (1989) 223.
[4] Z. Karpinski, Adv. Catal. 37 (1990) 45.
[5] N. Sheppard and C. de la Cruz, Adv. Catal. 41 (1996) 1.
[6] P.S. Cremer, S. Xingcai, Y.R. Shen and G.A. Somorjai, J. Am. Chem. Soc. 118 (1996) 2942.
[7] A. Cassuto, J. Kiss and J.M. White, Surf. Sci. 255 (1991) 289.
[8] P. Cremer, C. Stanners, J.W. Niemantsverdriet, Y.R. Shen and G. Somorjai, Surf. Sci. 328 (1995) 111.
[9] P.D. Szuromi, J.R. Engstrom and W.H. Weinberg, J. Phys. Chem. 89 (1985) 2497.
[10] M. Salmerón and G.A. Somorjai, J. Phys. Chem. 86 (1982) 341.
[11] P. Berlowitz, C. Megiris, J.B. Butt and H.H. Kung, Langmuir 1 (1985) 206.
[12] D. Godbey, F. Zaera, R. Yeates and G.A. Somorjai, Surf. Sci. 167 (1986) 150.
[13] R.G. Windham, M.E. Bartram and B.E. Koel, J. Phys. Chem. 92 (1988) 2862.
[14] R.G. Windham and B.E. Koel, J. Phys. Chem. 94 (1990) 1489.
[15] A. Stuck, C.E. Wartnaby, Y.Y. Yeo and D.A. King, Phys. Rev. Lett. 74 (1995) 578.
[16] B.E. Spiewak and J.A. Dumesic, Thermochim. Acta, accepted.
[17] B.E. Spiewak, R.D. Cortright and J.A. Dumesic, *Handbook of Heterogeneous Catalysis*, in press.
[18] S. Pálfi, W. Lisowski, M. Smutek and S. Cerny, J. Catal. 88 (1984) 300.
[19] H.A. Benesi, R.M. Curtis and H.P. Studer, J. Catal. 10 (1968) 328.
[20] N. Cardona-Martínez and J.A. Dumesic, J. Catal. 125 (1990) 427.
[21] S.A. Goddard, M.D. Amiridis, J.E. Rekoske, N. Cardona-Martínez and J.A. Dumesic, J. Catal. 117 (1989) 155.
[22] A.D. Becke, J. Chem. Phys. 98 (1993) 5648.
[23] W.J. Hehre, L. Radom and P. von R. Schleyer, *Ab Initio Molecular Orbital Theory* (Wiley, New York, 1986) ch. 4.
[24] T. Ziegler, Chem. Rev. 91 (1991) 651.
[25] W. Kohn, A.D. Becke and R.G. Parr, J. Phys. Chem. 100 (1996) 12974.
[26] M.J. Frisch, G.W. Trucks, H.B. Schlegel, P.M.W. Gill, B.G. Johnson, M.A. Robb, J.R. Cheeseman, T. Keith, G.A. Petersson, J.A. Montgomery, K. Raghavachari, M.A. Al-Laham, V.G. Zakrzewski, J.V. Ortiz, J.B. Foresman, J. Cioslowski, B.B. Stefanov, A. Nanayakkara, M. Challacombe, C.Y. Peng, P.Y. Ayala, W. Chen, M.W. Wong, J.L. Andres, E.S. Replogle, R. Gomperts, R.L. Martin, D.J. Fox, J.S. Binkley, D.J. Defrees, J. Baker, J.P. Stewart, M. Head-Gordon, C. Gonzalez and J.A.J.A. Pople, GAUSSIAN 94 (Revision C.2) (Gaussian Inc., Pittsburgh, 1995).
[27] C. Peng, P.Y. Ayala, H.B. Schlegel and M.J. Frisch, J. Comp. Chem. 17 (1996) 49.
[28] W.J. Hehre, L. Radom and P. von R. Schleyer, *Ab Initio Molecular Orbital Theory* (Wiley, New York, 1986) ch. 7.
[29] R.D. Cortright and J.A. Dumesic, J. Catal. 148 (1994) 771.

[30] P. Chou and M.A. Vannice, J. Catal. 104 (1987) 1.
[31] E. Wicke, H. Brodowsky and H. Züchner, in: *Hydrogen in Metals II*, Vol. 29, eds. G. Alefeld and J. Völkl (Springer, New York, 1978) ch. 3.
[32] R.G. Windham, B.E. Koel and M.T. Paffett, Langmuir 4 (1988) 1113.
[33] B.E. Spiewak, R.D. Cortright and J.A. Dumesic, to be published.
[34] M.T. Paffett, S.C. Gebhard, R.G. Windham and B.E. Koel, Surf. Sci. 223 (1989) 449.
[35] N.R. Avery and N. Sheppard, Proc. Royal Soc. A 405 (1986) 1.
[36] A. Cassuto and G. Tourillon, Surf. Sci. 307–309 (1994) 65.
[37] N.R. Avery, J. Catal. 19 (1970) 15.
[38] G. Shahid and N. Sheppard, Can. J. Chem. 69 (1991) 1812.
[39] L. Hammer, B. Dötsch, F. Brandenstein, A. Fricke and K. Müller, J. Electron. Spectrosc. Rel. Phen. 54/55 (1990) 687.
[40] C. Xu, B.E. Koel and M.T. Paffett, Langmuir 10 (1994) 166.
[41] W.H. Weinberg and Y. Sun, Surf. Sci. Lett. 277 (1992) L39.
[42] J.R. Anderson and N.R. Avery, J. Catal. 5 (1966) 446.
[43] G.C. Bond and M.R. Gelsthorpe, J. Chem. Soc. Faraday Trans. I 85 (1989) 3767.
[44] S.A. Goddard, M.D. Amiridis, J.E. Rekoske, N. Cardona-Martinez and J.A. Dumesic, J. Catal. 117 (1989) 155.
[45] G.C. Bond, R.H. Cunningham and E.L. Short, in: *Proc. 10th Int. Congr. on Catalysis* (Budapest l992), eds. L. Guczi, F. Solymosi and P. Tétényi (Adadémiai Kiadó, Budapest, 1993) p.130.
[46] R.D. Cortright and J.A. Dumesic, J. Catal. 157 (1995) 576.